

Comparison of Power Dependence of Microwave Surface Resistance of Unpatterned and Patterned YBCO Thin Film

H. Xin,^{†◇*} D. E. Oates,^{†◇} A. C. Anderson,[◇] R. L. Slattery,[◇] G. Dresselhaus,^{†*}
M. S. Dresselhaus[†]

[†] *Massachusetts Institute of Technology, Cambridge, MA 02139*

[◇] *Lincoln Laboratory, Lexington, MA 02420*

^{*} *AFRL, Hanscom AFB, Bedford, MA 01731*

(January 5, 2018)

Abstract

The effect of the patterning process on the nonlinearity of the microwave surface resistance R_S of YBCO thin films is investigated. With the use of a sapphire dielectric resonator and a stripline resonator, the microwave R_S of YBCO thin films was measured before and after the patterning process, as a function of temperature and the rf peak magnetic field in the film. The microwave loss was also modeled, assuming a J_{rf}^2 dependence of $Z_S(J_{rf})$ on current density J_{rf} . Experimental and modeled results show that the patterning has no observable effect on the microwave residual R_S or on the power dependence of R_S .

I. INTRODUCTION

The nonlinearity (power dependence) of the microwave (rf) surface impedance Z_S of the high- T_c superconductors is important for both practical applications and fundamental materials understanding. Nonlinearity in the surface impedance not only degrades the power handling ability of devices but also causes intermodulation and harmonic generation problems at moderate power levels. There has been a large amount of effort to investigate the nonlinear Z_S , but the origins of these phenomena are still not understood. Since most of the measurements have been performed on photolithographically patterned stripline or coplanar waveguide devices, one of the suggested explanations for the nonlinearity is defects and damage caused by patterning. All patterned devices have some current crowding near their edges. For example, stripline and microstrip devices have current distributions that peak sharply near their edges, where the patterning processes have a relatively large influence.

A SEM picture focusing on the edge of a patterned YBCO thin film is shown in Fig. 1. The edge is not straight as can be seen in the picture and the roughness of the edge is of the order of a superconducting penetration depth. This edge roughness results from the initial imperfections of the photoresist pattern and from nonuniformities of the etching process. The edge roughness led to the speculation that the condition of the YBCO line edge was influencing the power dependence, and this was the initial motivation for this work. The bright particles on the surface of the YBCO film are the well-known copper oxide outgrowths that are present in all films whose stoichiometry is not exact¹. We have found that outgrowths do not adversely affect the microwave properties and therefore it is unnecessary to make large efforts to deposit films with exactly the correct stoichiometry. We have also observed that improvement of the surface morphology to make smoother films than that shown in Fig. 1 does not improve their microwave properties either with regard to their residual R_S or their power dependence.

In the present work, we used both a sapphire dielectric resonator and a stripline resonator to directly compare the power dependence of the microwave surface resistance R_S of the *same* YBCO thin films, first unpatterned in the dielectric resonator and then patterned in the stripline resonator. Experimental procedures and results are shown in the following sections. To help understand our experimental results better, we have also modeled the R_S as measured in the dielectric resonator and in the stripline resonator using the following simple phenomenological assumption,

$$\rho(\vec{r}) = \rho_0 + \rho_2 J_{rf}(\vec{r})^2, \quad (1)$$

$$\lambda(\vec{r}) = \lambda_0 + \lambda_2 J_{rf}(\vec{r})^2 \quad (2)$$

where $\rho(\vec{r})$ and $\lambda(\vec{r})$ are, respectively, the real part of the complex local resistivity and penetration depth, $J_{rf}(\vec{r})$ is the local current density in the film, and ρ_2 and λ_2 are the corresponding nonlinear coefficients.

II. EXPERIMENTAL METHOD

In order to study the effects of defects and damage introduced in the patterning process on the power dependence of the microwave surface resistance of YBCO thin films, we

measured the nonlinear microwave frequency surface resistance at 10.7 GHz of unpatterned, 2-inch-diameter, YBCO films using a specially designed sapphire dielectric resonator. The unpatterned films were then patterned using standard photolithography and wet chemical etching with 0.1% phosphoric acid to make stripline resonators with resonant frequencies $f_0 = nf_1$, where $n = 1, 2, \dots$ and $f_1 = 1.5$ GHz. The patterning and dicing procedures are described in Fig. 2. The microwave surface resistance was then measured as a function of rf power for the patterned striplines. Comparing our results “before” and “after” the patterning process, directly clarifies whether the patterning contributes to the power dependence of the microwave surface resistance observed for YBCO thin films.

A. Sapphire Dielectric Resonator

We have designed a sapphire dielectric resonator shown in Fig. 3 to measure the microwave surface resistance and especially the power dependence of unpatterned YBCO thin films. The resonator incorporates some unique features described below that allow high-power measurements to be carried out without heating the sample via dissipated power. Figure 4 is a cut-away view of the dielectric resonator. The resonator was made from a $\frac{1}{2}$ -inch-diameter and $\frac{1}{4}$ -inch-high cylindrical sapphire puck that is grounded by two 2-inch-diameter YBCO wafers (see left hand side of Fig. 2). The resonator has fixed output coupling and in-situ-adjustable input coupling to ensure critical input coupling (no reflection at the input end) for high-power measurements. The resonator is packaged in an oxygen-free copper case, as shown in Fig. 3. Special thermal contacts were designed to avoid heating problems for high-power experiments. A copper pressure plate was employed on top of the upper YBCO wafer. Springs were used (as shown in Fig. 3) to ensure that the pressure on the YBCO is independent of temperature. A gold-plated copper foil was soldered onto the copper pressure plate to enhance thermal conduction to the copper case from the top YBCO film which was more likely to be affected by heating than the bottom wafer that was anchored to the copper base plate. Thermal-conducting grease was applied between the sapphire puck and the two grounding wafers. The whole package was operated in a vacuum environment in a cryocooler with the bottom plate bolted to the cold finger with an indium foil for thermal contact. A temperature sensor and a 25- Ω heater were mounted on the copper case of the resonator with indium foil to monitor and control the temperature.

The sapphire dielectric resonator was operated at the TE_{011} mode for which the center frequency was 10.7 GHz. The loaded quality factor Q_L , reflection (S_{11} , S_{22}) and transmission (S_{21}) coefficients were measured as a function of input power and temperature. The input coupling loop was tuned in-situ to maintain critical coupling at each temperature and input power level. Critical coupling on the input maximizes the circulating power and rf magnetic field in the resonator. The output coupling loop was fixed and weakly coupled during each measurement. The unloaded quality factor Q_0 was obtained from the measured S parameters and Q_L , and the surface resistance was deduced from $R_S = G/Q_0$, where G is the calculated geometric factor of the resonator.² The results for R_S are presented as a function of peak magnetic field in the resonator. The R_S measured by this method is the average of R_S in the top and bottom YBCO films.

The Q_L was measured using a standard frequency-domain 3-dB bandwidth method at a low input power where the Q is independent of power. At higher input power levels, a time-

domain method was employed to reduce heating effects. In this method, a CW microwave pulse with enough duration to fully charge the resonator was sent into the resonator. After the input pulse is turned off, we can calculate Q_L from the decay rate of the output signal that is proportional to $\exp[-\omega t/Q_L]$. By use of the time-domain method with this special thermal design, the R_S could be measured without heating problems for input powers up to 40 dBm, which corresponds to a rf peak magnetic field of ≥ 100 Oe. Surface resistance measurements on two pairs of unpatterned YBCO films were carried out for temperatures in the range 30 to 80 K.

In the analysis of the experimental data, we have, as is usual, treated the losses of the YBCO superconducting ground planes as a perturbation that does not affect the field or current distribution, while ignoring the losses due to the sapphire puck itself and to the copper case. The assumption that only the YBCO films contribute to the power loss is expected to be valid for the following reasons. A good-quality sapphire crystal is almost lossless at the cryogenic temperature where we operated, since the $\tan \delta$ (loss tangent) is estimated^{2,3} to be on the order of 10^{-9} . For YBCO films, a Q_0 of about 10^6 is observed at low temperatures. A pair of 2-inch-diameter Nb films have yielded Q_0 values greater than 5×10^6 . That the Nb films gave a higher Q than those of YBCO indicates that the loss in the sapphire puck is negligible compared to that of the YBCO films. We estimated that the loss in the copper case is very small and yields a Q greater than 2.5×10^8 , much higher than that of the YBCO films.

B. Stripline Resonator

After the microwave surface resistance of the unpatterned YBCO films was measured with the sapphire dielectric resonator, the films were patterned and stripline resonators were made. A standard patterning process with wet chemical etching was employed. As shown in Fig. 2, each 2-inch wafer was made into four striplines and four ground planes. One piece from each of the top and the bottom YBCO wafers used with the dielectric resonator in Fig. 3 was measured. A description of the stripline resonator used here can be found in detail elsewhere.^{4,5} Similar to the dielectric resonator method, the loaded quality factor Q_L was measured for the stripline as a function of microwave input power up to 35 dBm, corresponding to a rf peak magnetic field of 1000 Oe in the resonator. One advantage of the stripline resonator is that the R_S at different overtone frequencies can be easily measured. By measuring overtones, we could measure the Q at frequencies close to that of the dielectric resonator even though the fundamental resonance of the stripline resonator is 1.5 GHz.

III. EXPERIMENTAL RESULTS

The R_S as a function of rf peak magnetic field H_{\max} at different temperatures was measured for two pairs of unpatterned YBCO films, denoted as pair 1 and 2 (see Fig. 3). The results are shown in Fig. 5. For pair 1, no nonlinearity in R_S of the unpatterned wafers was observed up to 80 K even at +40 dBm, the maximum available power, and corresponding to H_{rf} values up to 200 Oe. As mentioned above, R_S obtained for the unpatterned wafers is an average surface resistance of the pair of films. Figure 6(a) compares R_S of the unpatterned

and patterned films at 35 K for pair 1. The open circles represent the R_S of the patterned film from the top wafer measured in the dielectric resonator, and the crosses denote the R_S of the patterned film from the bottom wafer. The average of those two curves (dashed line) agrees with the R_S of the unpatterned wafers very well and suggests that there is no nonlinearity for H_{\max} up to 500 Oe. Figure 6(b) shows the results at 75 K for pair 1. For the case of stripline resonators, because of package modes interfering with some of the overtone modes, the R_S could not be measured at the mode closest in frequency to that of the dielectric resonator. Therefore R_S was measured at the closest frequencies possible. The results for R_S were then scaled assuming $R_S \propto \omega^2$. For pair 1 the R_S of the unpatterned films was measured at 10.7 GHz, and the R_S of the two patterned films was measured at 12 GHz and 7.5 GHz.

From the results in Fig. 6, we conclude that for pair 1, no degradation in the residual surface resistance was observed in the patterned stripline films up to a H_{\max} of ~ 200 Oe. No power dependence was observed up to the maximum input power available for the unpatterned films, and no effects of patterning on the power handling of YBCO films could be found either at 35 K or at 75 K for pair 1.

We grew another pair of 2-inch-diameter YBCO wafers pair 2, under a different deposition temperature with the intention to decrease the power handling of the microwave surface resistance. For pair 2 at 35 K no power dependence of the R_S was observed in the dielectric resonator up to the maximum input power, similar to the results obtained for pair 1. However, at $T = 75$ K, a nonlinearity in the R_S was observed above $H_{\max} \sim 100$ Oe. Results for the patterned films are shown together with that of the unpatterned films in Fig. 7. In this case, R_S was measured at 7.5 GHz for both patterned films in the stripline resonator. The measured residual surface resistance of the unpatterned and patterned films agrees to within 10%. The $R_S(H_{\max})$ for the unpatterned films actually turns up at a somewhat lower H_{\max} than for the patterned films in the stripline resonator. The apparently better power handling of the stripline resonator can be explained using the same surface impedance by a simple model introduced below. The H_{\max} is the rf peak magnetic field in the two types of resonators, but the two types of resonators have very different field distributions. In the next section, we use the different current/field profiles for both the sapphire dielectric and stripline resonators to model the measured power dependence of the unpatterned and patterned films.

IV. MODEL

The current profiles in the films for the dielectric and stripline resonators are different, as shown in Fig. 8. For the dielectric resonator with a film diameter much larger than the diameter of the sapphire puck so that the edge effects can be ignored, the current density \vec{J} is in the ϕ direction and has a dependence on radius given by^{2,6}

$$J(r) = \frac{H(r)}{\lambda_0} = \begin{cases} A \frac{\beta}{\xi_1 \lambda_0} J_1(\xi_1 r) & \text{for } 0 < r < a \\ A \frac{\beta}{\lambda_0 \xi_2} \frac{J_0(\xi_1 a)}{K_0(\xi_2 a)} K_1(\xi_2 r) & \text{for } a < r < R \end{cases} \quad (3)$$

where J_0 , J_1 , K_0 , K_1 are various Bessel functions, β , ξ_1 and ξ_2 are constants determined by the geometry of the resonator, a is the radius of the sapphire puck and R is the radius of the

superconducting films. The current density thus peaks near the center of the film as shown in Fig. 8. For the stripline resonator, the current density \vec{J} has been calculated numerically in Ref 7. For the purpose of simplicity in the calculation, we approximated $J(x)$ with the following analytical form,⁸

$$J(x) = \begin{cases} J_s(0)[1 - (\frac{2x}{w})^2]^{-\frac{1}{2}} & x \ll w \\ J_s(0)(\frac{1.165}{\lambda_0})(wb)^{\frac{1}{2}} \exp(-\frac{(w/2-|x|)b}{\lambda_0^2}) & x \approx w \end{cases} \quad (4)$$

where, w and b are, respectively, the width and thickness of the film. This analytical approximation agrees with the numerically calculated current distribution to within 5% in our case. Thus $J(x)$ peaks sharply at the edges of the patterned film for the stripline resonator. For the dielectric resonator, as is obvious in Eq. (3), $J(x)$ is related directly to the rf peak magnetic field H_{\max} . For the stripline resonator, H_{\max} can be calculated numerically from the current distribution in the stripline.⁷ For the same maximum field H_{\max} in the dielectric and stripline resonators, the portion of the film carrying a high current density is larger for the dielectric resonator due to the broader peak in the $J(r)$ distribution of the dielectric resonator. Therefore an apparently better power handling in the stripline resonator is not surprising.

The quality factors $Q_0(H_{\max})$ and in turn $R_S(H_{\max})$ of both resonators have been modeled as a function of rf peak magnetic field using the current distributions given above, with the assumption for the impedance is given by Eqs. (1) and (2), and

$$Q_0 = \omega \frac{W_{\text{stored}}}{P_{\text{diss}}}, \quad (5)$$

where W_{stored} is the total energy stored and P_{diss} is the power dissipated in the resonator. The parameters ρ_0 and λ_0 were taken from experimentally measured values, $\rho_0 = 7.2 \times 10^{-11} \Omega\text{m}$, $\lambda_0 = 0.2 \mu\text{m}$, that fit the low-field, linear part of R_S and the temperature dependence of the resonant frequency. The nonlinear parameters of resistivity and penetration depth used in the calculations in the superconducting phase were $\rho_2 = 1.0 \times 10^{-35} \Omega\text{m}^5/\text{A}^2$ and $\lambda_2 = 2.5 \times 10^{-29} \text{m}^5/\text{A}^2$. These parameters were taken to fit the R_S obtained from the dielectric resonator measurements. The unloaded quality factor for the stripline resonator was then calculated with the same set of parameters. At low rf field, calculated values of Q_0 of 7×10^5 and 6000, respectively, were obtained for the dielectric and stripline resonators, and these values are consistent with the measured values. The modeled results also show that the power dependence of R_S for both the dielectric and stripline resonators is quantitatively consistent with the measured power dependence for both resonators. The modeled R_S of the dielectric resonator turns up at a smaller value of H_{\max} than that of the stripline resonator, which agrees with the experimental result well as shown in Fig. 9.

V. CONCLUSIONS AND DISCUSSION

We have measured the microwave surface resistance of the *same* YBCO thin films, before and after patterning, using a sapphire dielectric resonator and a stripline resonator. A phenomenological model of the $R_S(H_{\max})$ in the two cases is presented. Based on this model, the calculated results fit the experimental data well in both cases using the same

materials parameters. Therefore, we conclude that our results are consistent with no damage or degradation of the power dependence of the microwave surface resistance due to the patterning of the films. The procedure described in this paper can also be used to test other patterning processes such as ion beam etching, etc.

ACKNOWLEDGMENTS

This work was supported by the Air Force Office of Scientific Research. The authors express their gratitude to Bob Koneizcka and Earle Macedo for applying their tireless efforts and effective skills to the preparation of the devices used in this study, and to Peter Murphy for providing the SEM pictures used in this study.

REFERENCES

- ¹ A. C. Westerheim, P. C. McIntyre, S. N. Basu, D. Bhatt, L. S. Yu-Jahnes, A. C. Anderson, and M. J. Cima. “Comparison of the Surface Morphology and Microstructure of In Situ and Ex Situ Derived $YBa_2Cu_3O_{7-x}$ Thin Films”. *Journal of Electronic Materials*, vol. 22, pp. 1113–1120, 1993.
- ² Z. Y. Shen, C. Wilker, P. Pang, W. L. Holstein, D. Face, and D. J. Kountz. “High- T_c Superconductor-Sapphire Microwave Resonator with Extremely High Q-Values up to 90 K”. *IEEE Trans. of Applied Superconductivity*, vol. 40, pp. 2424–2431, 1991.
- ³ D. G. Blair and A. M. Sanson. “High Q Tunable Sapphire Loaded Cavity Resonator for Cryogenic Operation”. *Cryogenics*, vol. 29, pp. 1045–1049, 1989.
- ⁴ D. E. Oates, A. C. Anderson, and P. M. Mankiewich. “Measurements of the Surface Resistance of $YBa_2Cu_3O_{7-x}$ Thin Films in Stripline Resonators”. *J. Supercond.*, vol. 3, pp. 251–259, 1990.
- ⁵ D. E. Oates, P. P. Nguyen, G. Dresselhaus, M. S. Dresselhaus, C. W. Lam, and S. M. Ali. “Measurements and Modeling of Linear and Nonlinear Effects in Striplines”. *J. Superconduct.*, vol. 5, pp. 361–369, 1992.
- ⁶ D. Kajfez and P. Guillon. *Dielectric Resonators*. Artech House Inc., New York, NY, 1986.
- ⁷ D. M. Sheen, S. M. Ali, D. E. Oates, R. S. Withers, and J. A. Kong. “Current Distribution, Resistance and Inductance for Superconducting Strip Transmission Lines”. *IEEE Trans. Appl. Supercond.*, vol. 1, pp. 108–115, 1991.
- ⁸ T. van Duzer and C. W. Turner. *Principles of Superconductive Devices and Circuits*. Elsevier North Holland, Inc., New York, NY, 1981.

FIGURES

FIG. 1. A SEM picture of the edge of a patterned YBCO stripline.

FIG. 2. YBCO film before(left) and after(right) the patterning and dicing processes.

FIG. 3. Structure of the dielectric resonator.

FIG. 4. Cut-away view of the dielectric resonator.

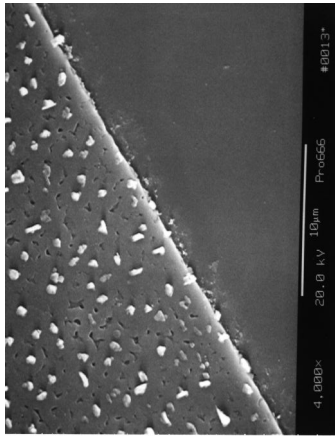
FIG. 5. R_S vs. rf peak magnetic field(H_{max}) for the unpatterned films (pair 1) for various temperatures.

FIG. 6. R_S vs. rf peak magnetic field(H_{max}) for both unpatterned and patterned films (pair 1) at (a) 35 K and (b) 75 K. The solid circles represent data of the unpatterned films; the open circles and crosses represent data of the patterned films from the top and bottom wafers, respectively; the dashed line represents the average R_S of patterned films from the top and bottom wafers.

FIG. 7. R_S vs. rf peak magnetic field for both unpatterned wafers 1 and 2 and the patterned films (pair 2) at 75 K. The squares represent data of the unpatterned films; the circles and the triangles represent data of the patterned films from the top and bottom wafers, respectively.

FIG. 8. Current distributions of both the stripline resonator (left) and the dielectric (sapphire) resonator (right).

FIG. 9. Modeled and measured R_S vs. rf peak magnetic field for both the dielectric resonator and the stripline resonator. The triangles represent the measured R_S for the dielectric resonator; the circles represent the measured R_S for the stripline resonator; the dashed line represents the modeled R_S for the dielectric resonator; the solid line represents the modeled R_S for the stripline resonator.

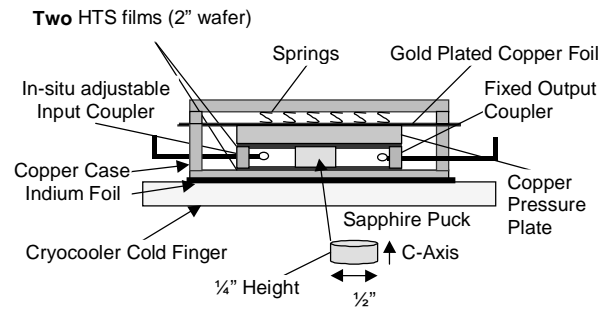


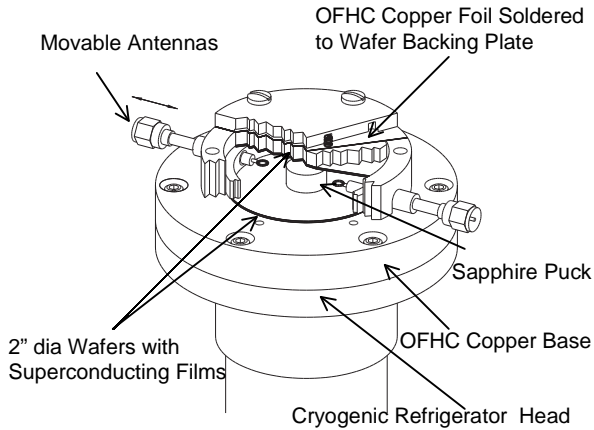


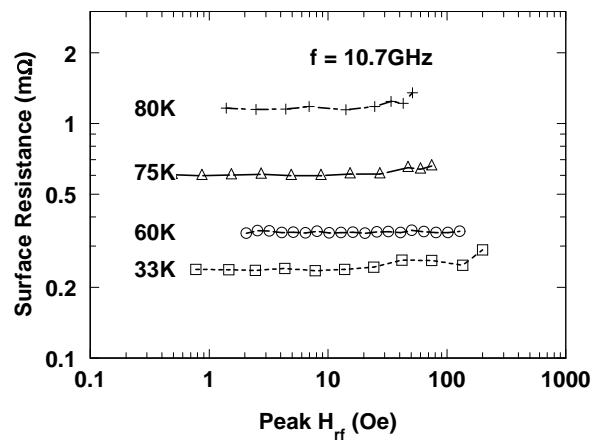
**Patterning + dicing
process**

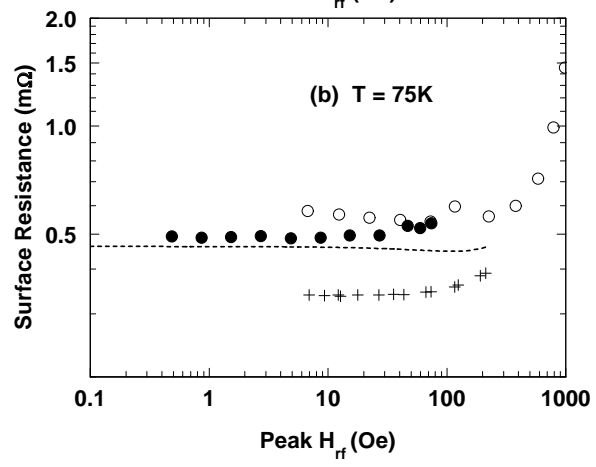
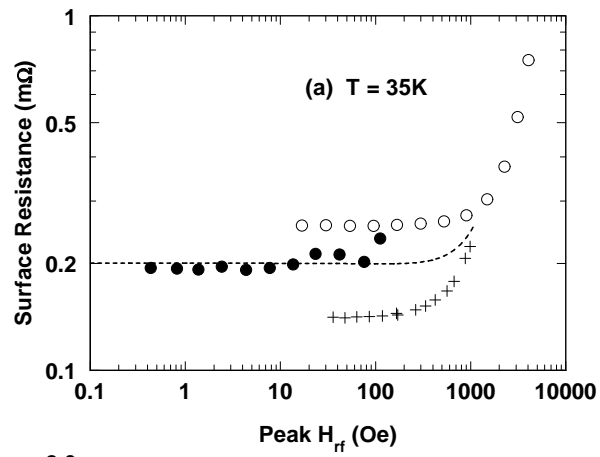
Unpatterned 2" diameter
YBCO film

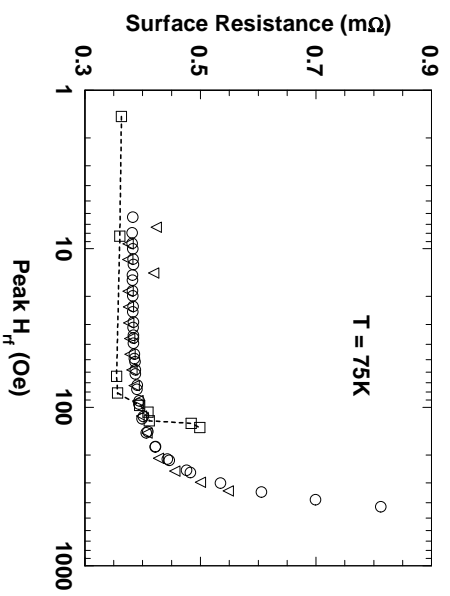
Patterned striplines



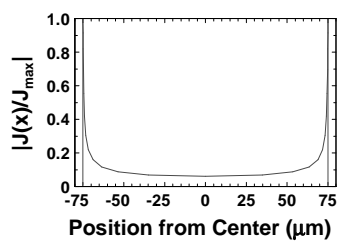




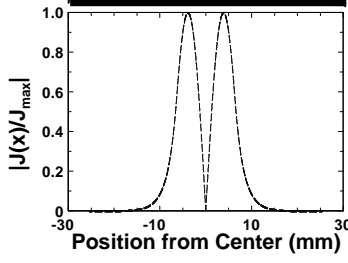
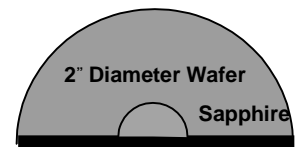




Stripline Cross Section



$J_{max} \sim 1.6 \times 10^8 \text{ A/cm}^3$



$J_{max} \sim 4.0 \times 10^6 \text{ A/cm}^3$

